Sequential release of drugs from dual-delivery plasmonic nanogels containing lipid-gated mesoporous silica-coated gold nanorods

Filipa Costa-e-Sá,[a,b] María Comís-Tuche,[c] Carlos Spuch,[c] Elisabete M. S. Castanheira,[a,b] and Sérgio R. S. Veloso[a,b,*]

[a] Physics Centre of Minho and Porto Universities (CF-UM-UP), University of Minho, Campus de Gualtar, 4710-057 Braga, Portugal.
[b] LaPMET Associate Laboratory, University of Minho, Campus de Gualtar, 4710-057 Braga, Portugal.
[c] Translational Neuroscience Research Group, Galicia Sur Health Research Institute (IIS-Galicia Sur), SERGAS-UVIGO, CIBERSAM, Vigo, Spain.

* Correspondence: sergioveloso96@gmail.com;

Supplementary Material

Fluorescence emission calibration curves of methotrexate and doxorubicin

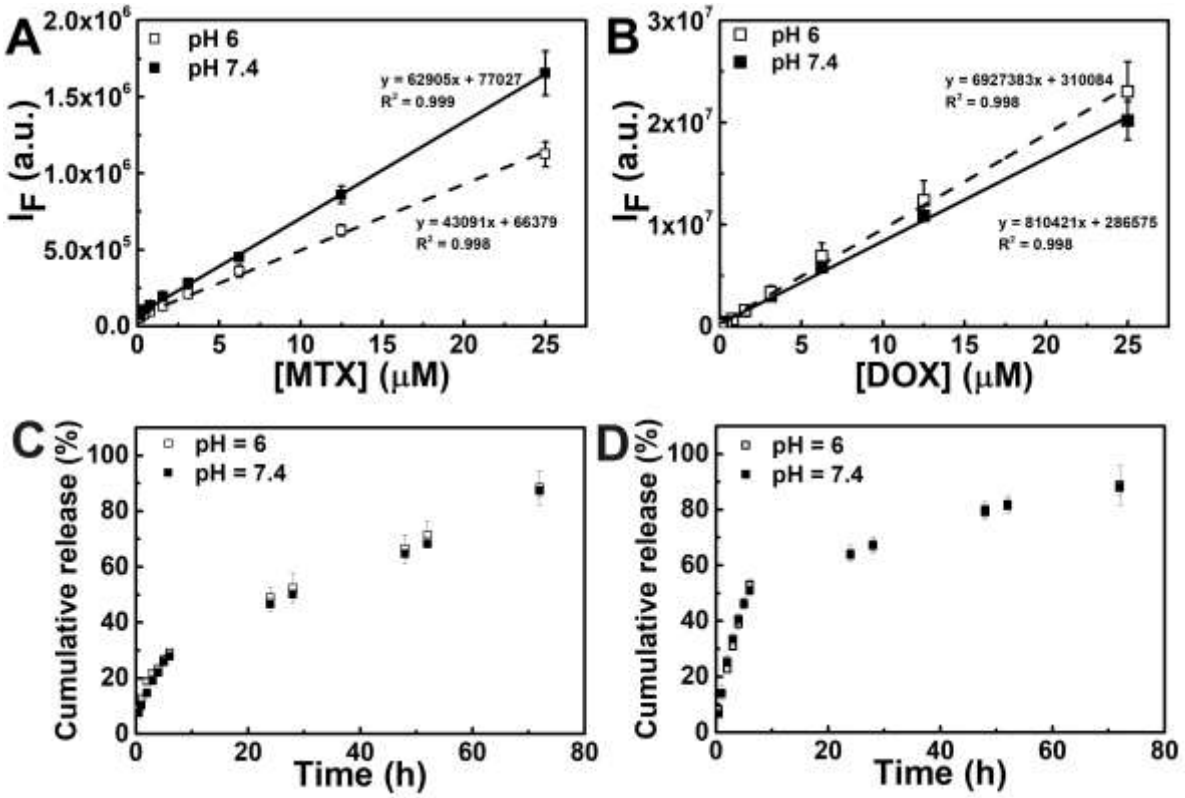

Figure S1. Fluorescence emission calibration curves of (A) methotrexate (λ_{exc} = 370 nm; λ_{em} = 460 nm) and (B) doxorubicin (λ_{exc} = 480 nm; λ_{em} = 598 nm) in pH 6 and pH 7.4. Release profiles of free (C) MTX and (D) DOX at pH 6 and pH 7.4.

Table S1. Limited-of-detection (LOD) and limit-of-quantification (LOQ) obtained from the calibration curves of MTX and DOX at pH 6 and 7.4.

Drug	pH	LOD (μM)	LOQ (μM)
MTX	6	0.54	1.63
	7.4	0.33	0.99
DOX	6	0.63	1.91
	7.4	0.53	1.62

Characterization of the lipid-gated mesoporous silica-coated gold nanorods

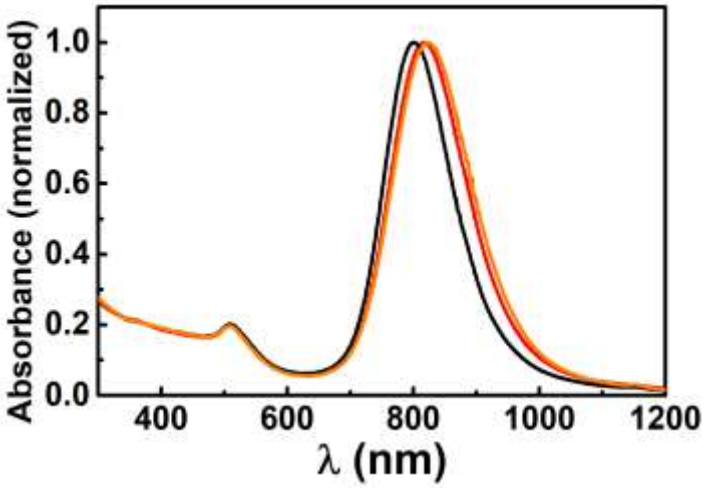

Figure S2. UV/Vis/NIR absorption spectra of different gold nanorod batches obtained by the same synthesis method. An average LSPR-to-TSPR of 5.05 ± 0.06 was obtained. The average LSPR maximum wavelength was 814 ± 9 nm.

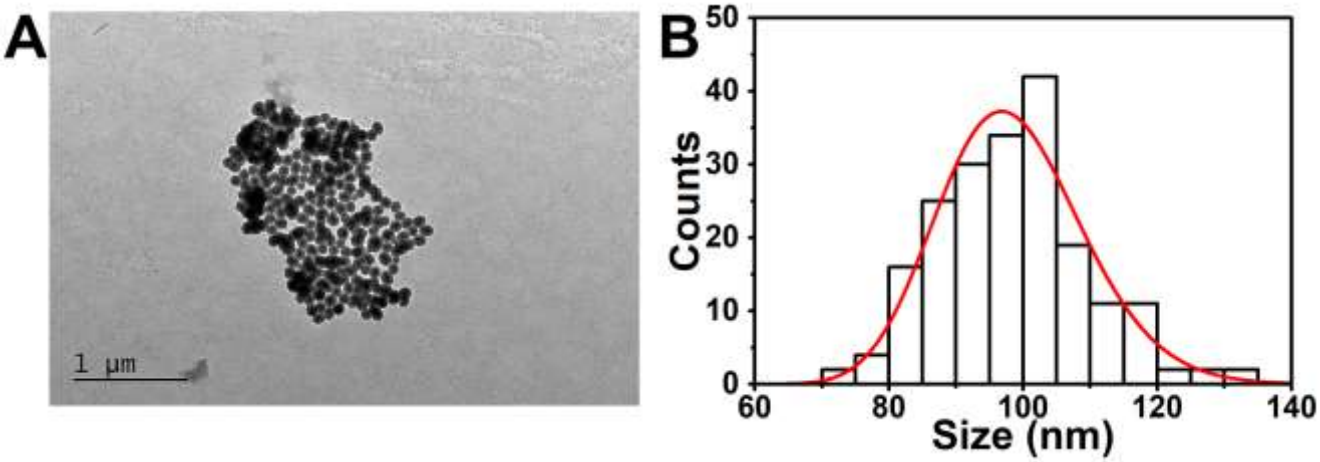

Figure S3. (A) TEM image of the synthesised mesoporous silica-coated gold nanorods and (B) the respective size histogram.

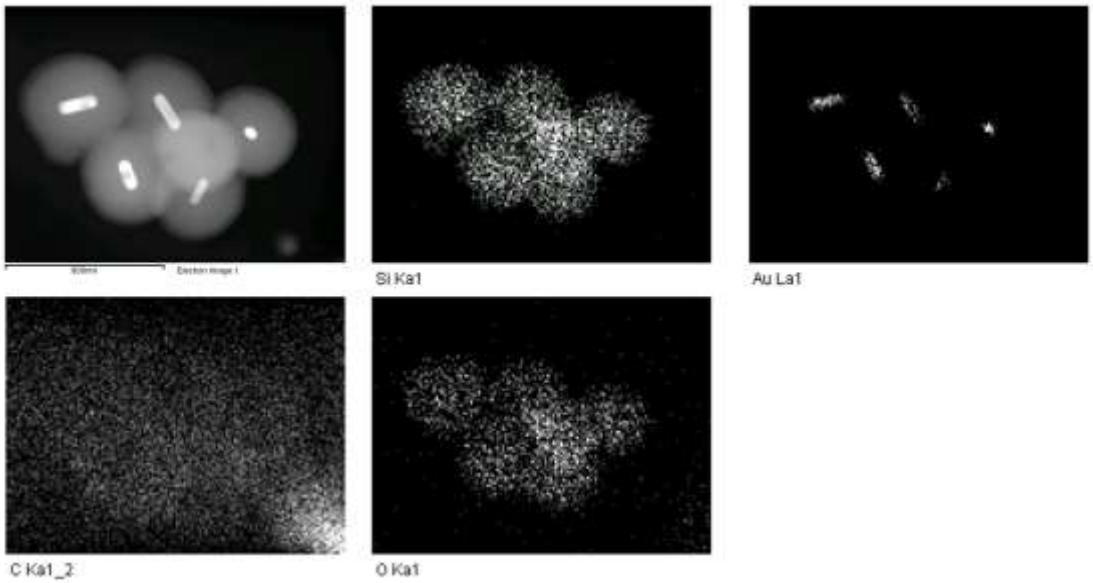

Figure S4. TEM image and EDS mapping of mesoporous silica-coated gold nanorods.

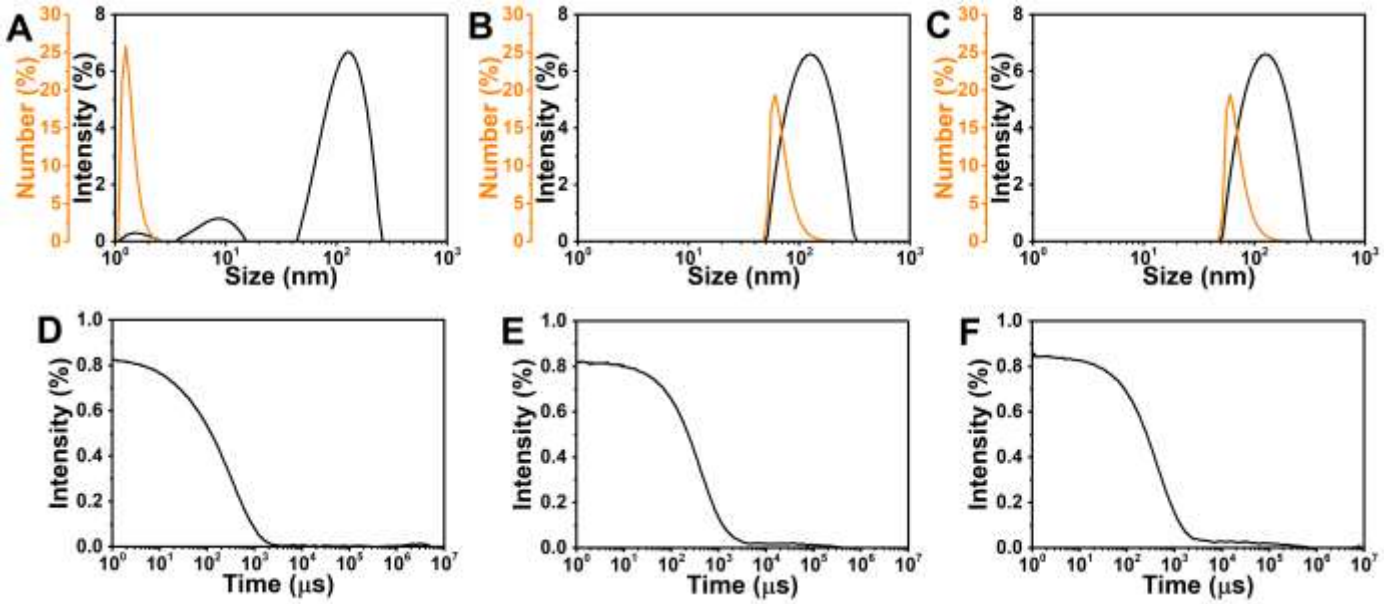

Figure S5. Dynamic light scattering intensity-weighted (black) and number-weighted (orange) distributions of (A) gold nanorods, (B) mesoporous silica-coated gold nanorods, (C) lipid-gated mesoporous silica-coated gold nanorods, and (D-F) respective correlograms.

Table S2. Hydrodynamic diameter (D_H), polydispersity and zeta potential of the gold nanorods (NR) with mesoporous silica shell (NR@Si) and gated with phospholipid membrane (NR@Si@Lip).

Nanoparticle	D_H (nm)	PDI	Zeta potential (mV)
NR	97 ± 1	0.27 ± 0.01	87 ± 3
NR@Si	132 ± 9	0.27 ± 0.01	-35 ± 1
NR@Si@Lip	144 ± 5	0.22 ± 0.01	-17 ± 1

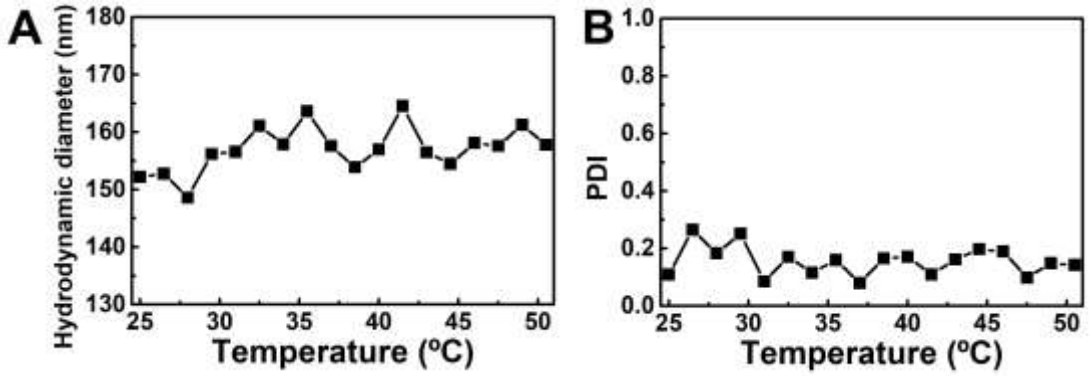

Figure S6. Dependence on temperature of the (A) hydrodynamic size, and (B) polydispersity of lipid-gated mesoporous silica-coated gold nanorods.

Characterization of the plasmonic nanogels

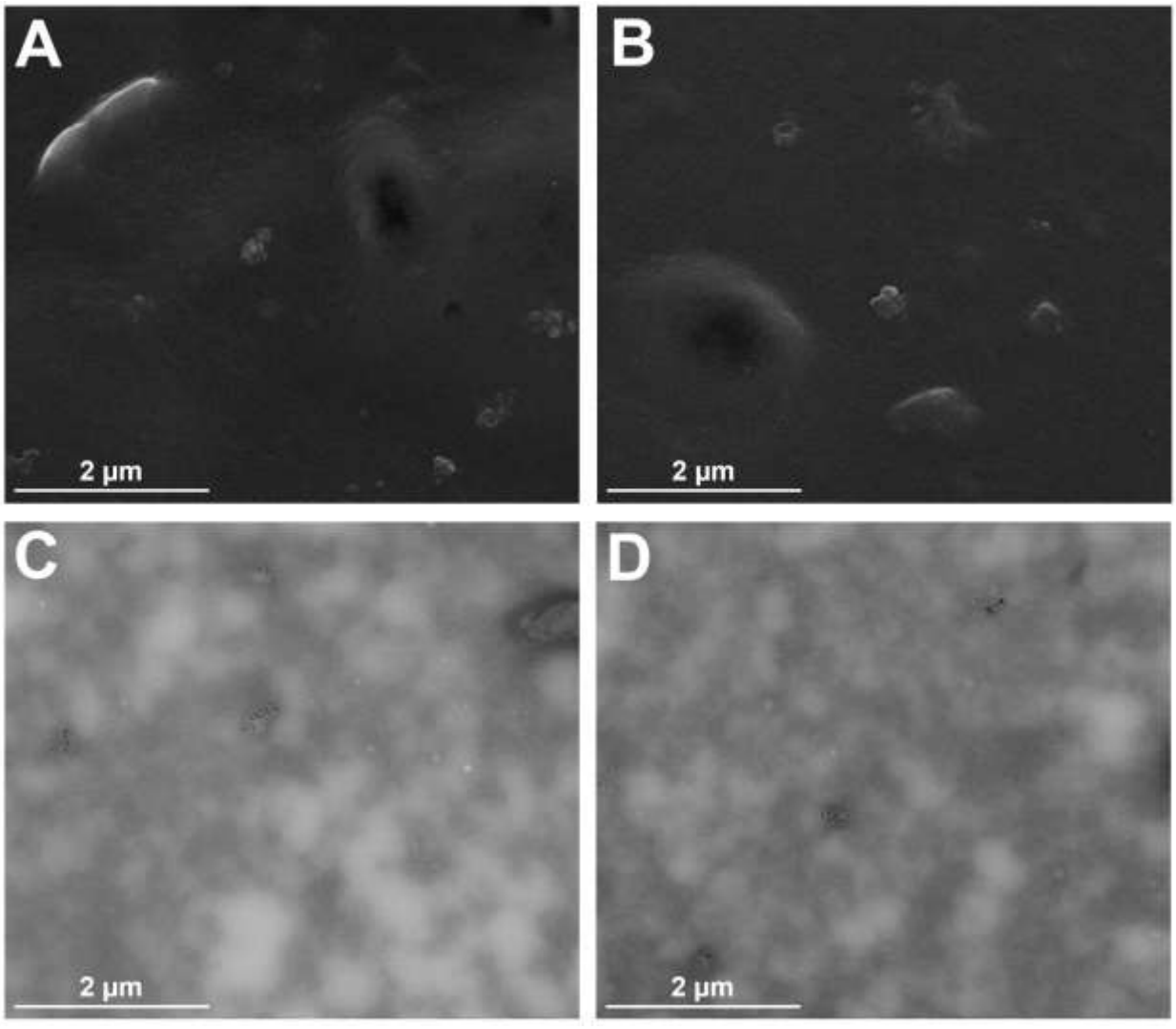

Figure S7. (A,B) SEM and (C,D) TEM images of plasmonic nanogels.

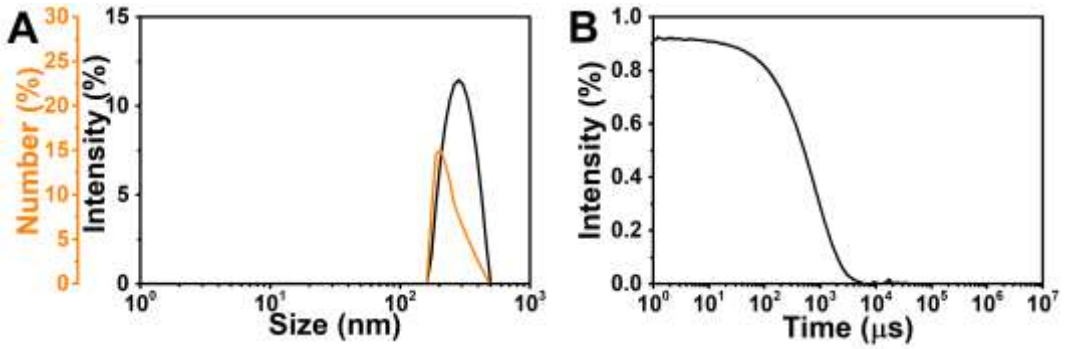

Figure S8. (A) Dynamic light scattering intensity-weighted (black) and number-weighted (orange) distributions of plasmonic nanogels, and (B) the respective correlogram.

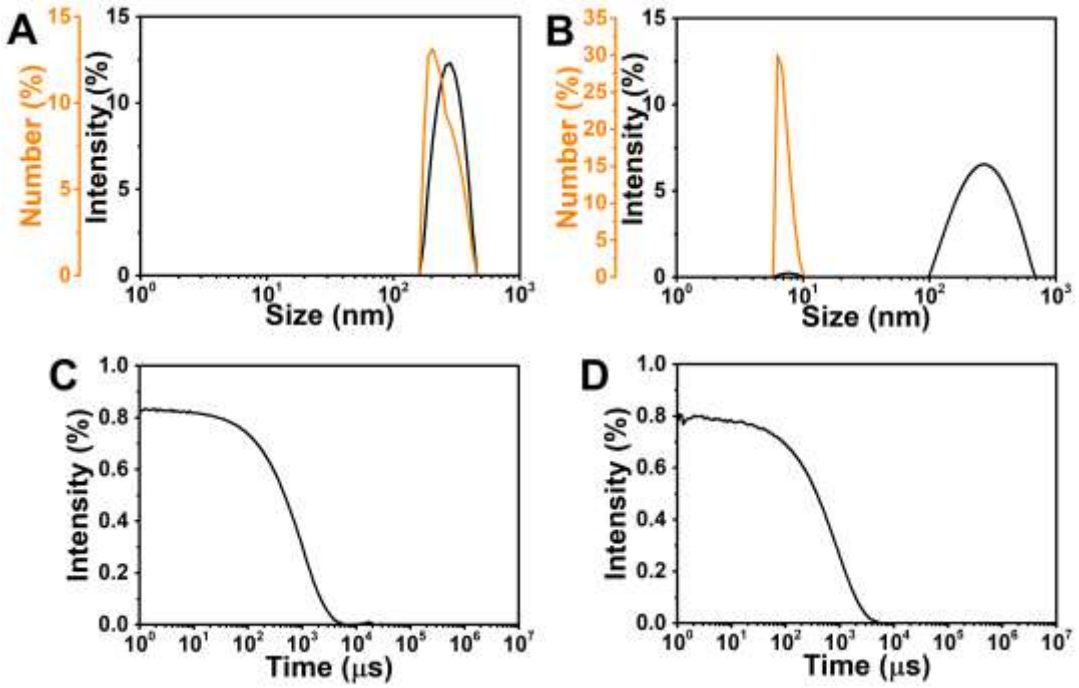

Figure S9. Dynamic light scattering intensity-weighted (black) and number-weighted (orange) distributions of plasmonic nanogels (A) before and (B) after six cycles of 3 min irradiation with 808 nm laser (1 W/cm^2), and (C,D) the respective correlograms.

Characterization of the drug-loaded plasmonic nanogels

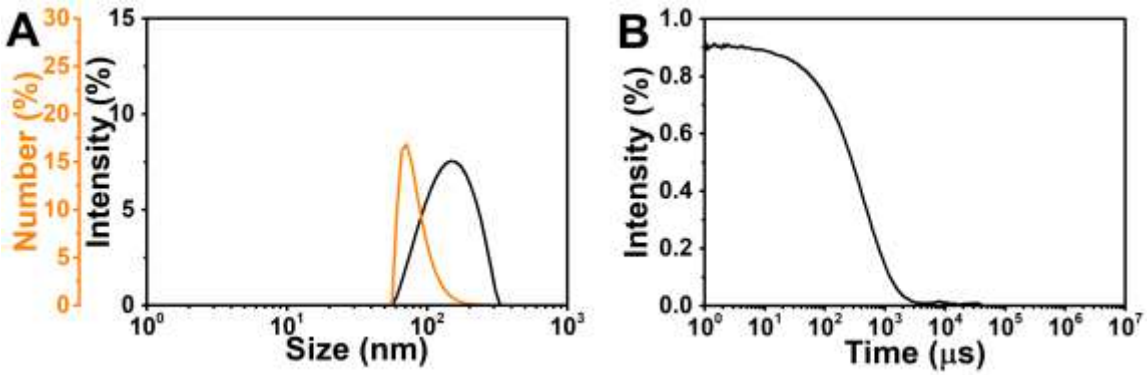

Figure S10. (A) Dynamic light scattering intensity-weighted (black) and number-weighted (orange) distributions of NR@Si@Lip loaded with MTX (1:1 NR:MTX) and (B) the respective correlogram.

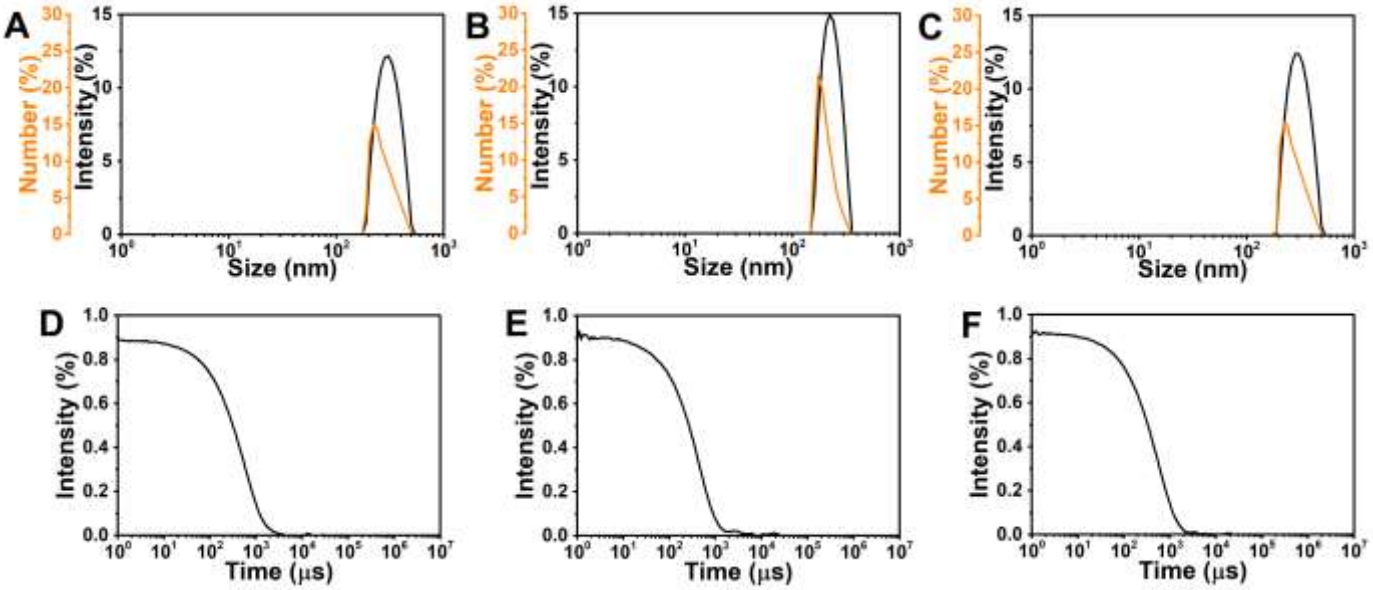

Figure S11. Dynamic light scattering intensity-weighted (black) and number-weighted (orange) distributions of plasmonic nanogels loaded with (A) doxorubicin, (B) methotrexate, (C) doxorubicin and methotrexate, and (D-F) the respective correlograms.

Drug release assays

Table S3. Coefficients of determination (R^2) of several fitted models obtained for methotrexate (MTX) and doxorubicin (DOX) release profiles in plasmonic nanogels. The blank spaces correspond to negative coefficients. The mathematical models were fitted to the 76 h release profiles.

Drug	pH	Stimuli	First-order	Hixson-Crowell	Higuchi	Korsmeyer-Peppas	Gompertz
MTX	6	-	0.73	-	0.66	0.97	0.97
		Laser	0.84	-	0.71	0.87	0.71
	7.4	-	0.82	-	0.70	0.93	0.86
		Laser	0.89	0.09	0.71	0.84	0.58
DOX	6	-	0.86	0.49	0.94	0.96	0.97
		Laser	0.78	0.22	0.84	0.93	0.96
	7.4	-	0.84	0.43	0.94	0.96	0.97
		Laser	0.89	0.63	0.96	0.97	0.98

The Gompertz and Korsmeyer-Peppas models are, respectively, described according to the equations:

$$X_t = X_{max} e^{-ae^{b \log_{10} t}} \quad \text{(S1)}$$

$$\frac{M_t}{M_\infty} = K_s t^n \quad \text{(S2)}$$

in which $\frac{M_t}{M_\infty}$ is the fraction of drug released at time t, and K_s is the rate constant. For a spherical geometry, when $n < 0.43$, the release mechanism is diffusion-controlled (Fickian diffusion), $0.43 < n < 0.85$ is an anomalous transport, and $n \geq 0.85$ indicates that the release is mainly driven by swelling or relaxation of network chains (case-II transport) [2,3]. The X_t and X_{max} are the dissolved drug fractions at time t and its maximum, a is a shape parameter and b is the dissolution rate per unit of time.

Table S4. Release coefficients of the Korsmeyer-Peppas and Gompertz models obtained for methotrexate (MTX) and doxorubicin (DOX) release profiles in plasmonic nanogels. The Korsmeyer-Peppas model was fitted to the initial 60% of the drug release profile. The parameter X_{max} of the Gompertz model was fixed at value 1.

			Korsmeyer-Peppas			Gompertz			
Drug	pH	Stimuli	K_S (h^{-1})	n	R^2	X_{max}	a	b	R^2
MTX	6	-	0.006	0.40	0.99	1	5.01	0.15	0.97
		Laser	0.011	0.29	0.99	1	4.74	0.23	0.71
	7.4	-	0.010	0.27	0.99	1	4.72	0.19	0.86
		Laser	0.014	0.28	0.99	1	4.71	0.31	0.58
DOX	6	-	0.019	1.03	0.99	1	3.47	0.52	0.97
		Laser	0.035	0.98	0.99	1	2.79	0.55	0.96
	7.4	-	0.004	0.98	0.99	1	5.02	0.281	0.97
		Laser	0.003	1.04	0.99	1	5.25	0.33	0.98

References

[1] S.R.S. Veloso, V. Gomes, S.L.F. Mendes, L. Hilliou, R.B. Pereira, D.M. Pereira, P.J.G. Coutinho, P.M.T. Ferreira, M.A. Correa-Duarte, E.M.S. Castanheira, Plasmonic lipogels: driving co-assembly of composites with peptide-based gels for controlled drug release, Soft Matter. 18 (2022) 8384–8397. https://doi.org/10.1039/D2SM00926A.

[2] P.L. Ritger, N.A. Peppas, A simple equation for description of solute release II. Fickian and anomalous release from swellable devices, J. Control. Release. 5 (1987) 37–42. https://doi.org/10.1016/0168-3659(87)90035-6.

[3] S. Dash, P.N. Murthy, L. Nath, P. Chowdhury, Kinetic modeling on drug release from controlled drug delivery systems, Acta Pol. Pharm. - Drug Res. 67 (2010) 217–223.